THE JOURNAL OF PHYSICAL CHEMISTRY C

Article

pubs.acs.org/JPCC

Fundamental Strategy for Creating VLS Grown TiO_2 Single Crystalline Nanowires

Fuwei Zhuge,[†] Takeshi Yanagida,*[,†] Kazuki Nagashima,[†] Hideto Yoshida,[†] Masaki Kanai,[†] Bo Xu,[†] Annop Klamchuen,[†] Gang Meng,[†] Yong He,[†] Sakon Rahong,[†] Xiaomin Li,[‡] Masaru Suzuki,[§] Shoichi Kai,[§] Seiji Takeda,[†] and Tomoji Kawai*[,†]

[†]The Institute of Scientific and Industrial Research, Osaka University, 8-1 Mihogaoka Ibaraki, Osaka, 567-0047, Japan

[‡]State Key Laboratory of High Performance Ceramics and Superfine Microstructures, Shanghai Institute of Ceramics, Chinese Academy of Sciences, Shanghai 200050, P. R. China

[§]Department of Applied Quantum Physics and Nuclear Engineering, Faculty of Engineering, Kyushu University, 744 Motooka, Nishi-ku, Fukuoka 819-0395, Japan

ABSTRACT: A single crystalline TiO_2 nanowire grown by a size and position controllable vapor−liquid−solid (VLS) method is a promising candidate to control and design the physical and chemical properties for various TiO_2-based applications. However, creating TiO_2 nanowires by VLS has been a challenging issue due to a difficulty on controlling and understanding the complex material transport events across three phases. Here we propose a fundamental strategy to create a TiO_2 single crystalline nanowire by the VLS mechanism. We show that a VLS growth of TiO_2 nanowires can emerge intrinsically only within a quite narrow range of material flux, which is a sharp contrast to typical VLS oxides including MgO, SnO_2, In_2O_3, and ZnO, whose nanowires are easily grown by VLS with much wider ranges of material flux. We reveal that a condensation of Ti atoms at a vapor−solid interface, which is detrimental for VLS, is responsible to limit a window of material flux for TiO_2 nanowires. In addition, we found that our rutile-TiO_2 nanowires preferentially grow along ⟨001⟩ direction, which interestingly differs from a typical ⟨110⟩ oriented growth of TiO_2 nanowires formed by the vapor-phase method. The present approach based on a control of material flux provides a foundation to tailor VLS grown TiO_2 nanowires based on a scientific strategy rather than a rule of thumb.

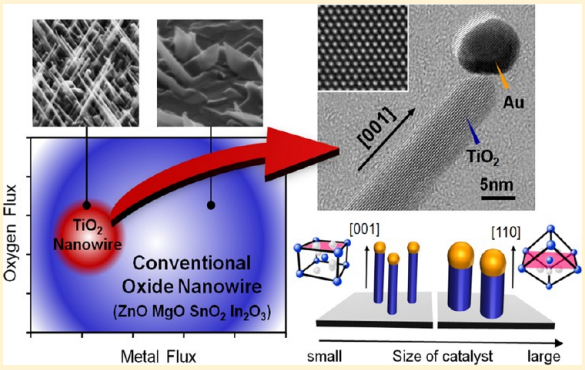

INTRODUCTION

Titanium dioxide (TiO_2) has shown a great promise for various applications, including e.g. photocatalyst, dye-sensitized solar cells, and water splitting systems.[1−4] Since the functionalities strongly rely on an electron transfer event at a surface of TiO_2, various TiO_2 nanostructures, including nanoparticles, nanoporous structures, and nanowires, have been proposed to enhance a device performance via increasing a surface area.[5] Among such TiO_2 nanostructures, a single crystalline 1D nanowire is especially an attracting candidate because this nanostructure essentially allows us to avoid a detrimental degradation of carrier mobility via reducing grain boundaries, at which a carrier tends to scatter.[6,7] There are various methods to fabricate TiO_2 nanowires. Among them, a hydrothermal method has most successfully fabricated 1D TiO_2 nanostructures.[8−13] Although hydrothermal methods are very attractive due to the applicability for various substrates, they often suffer from suppressing detrimental crystal defects due to the low-temperature process.[14] In addition, controlling intentionally the size ranges of diameter/length or the spatial locations seems to be unfeasible for hydrothermal synthesis. A size and position controllable VLS method for fabricating a nanowire is a promising to overcome above issues. Although a few reports have demonstrated the occurrence of a VLS growth for TiO_2 nanowires,[13,15,16] knowledge to create single crystalline TiO_2 nanowires by VLS has been substantially limited due to the lack of understanding the complex material transport events of VLS across three phases. Here we demonstrate a fundamental strategy to realize a TiO_2 single crystalline nanowire by VLS mechanism. We found that a VLS growth of TiO_2 nanowires can emerge intrinsically only within a quite narrow range of material flux. Interestingly, our rutile-TiO_2 nanowires preferentially grow along ⟨001⟩ direction, which differs from a typical ⟨110⟩ oriented growth in TiO_2 nanowires formed by the vapor-phase method.

Received: September 8, 2012
Revised: October 27, 2012
Published: October 29, 2012

 © 2012 American Chemical Society dx.doi.org/10.1021/jp308945b | J. Phys. Chem. C 2012, 116, 24367−24372

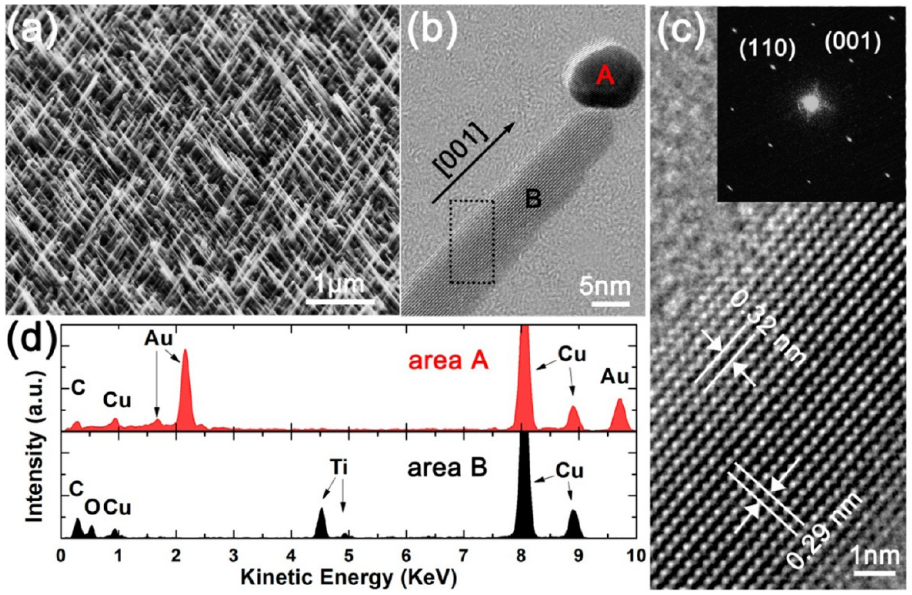

Figure 1. (a) SEM image of succsesufully fabricated TiO_2 nanowires grown on a sapphire (110) substrate. The image of 60° tilted angle is shown. (b) TEM image of fabricated TiO_2 nanowire with the Au catalyst at the tip. (c) HRTEM and SAED data of the selected area depicted in the dashed line within (b). A growth direction [001] is indicated. (d) EDS data at the selected position A and B in (b). Cu peaks are due to the use of Cu mesh for TEM analysis. This indicates the occurrence of VLS growth by showing the composition of Au catalysts.

EXPERIMENTAL SECTION

Nanowire Fabrication. We have fabricated TiO_2 nanowires by utilizing a pulse laser deposition technique with Au metal catalysts. The details of fabrication systems can be seen in elsewhere.[17−25] TiO_2 nanowires were fabricated onto a sapphire (110) and TiO_2 (001) or (110) single crystalline substrates (Crystal Base Co. Ltd.). Before the nanowire growth, an Au thin layer (~1 nm) was deposited onto a substrate by dc sputtering. To supply a vapor source of Ti atom, a Ti metal target (~99.9% purity) was utilized, which was ablated by ArF excimer laser (λ = 193 nm). The ablation area and frequency were 0.02 cm^2 and 10 Hz, respectively, while the laser energy was changed from 40 to 80 mJ to vary the material flux of Ti. The material flux of oxygen was varied by changing an oxygen partial pressure ranged from 10^{-4} to 1 Pa in the mixed gas of O_2 and Ar under the constant total pressure of 10 Pa. The use of constant total pressure is important to keep identical transport kinetics of Ti species to the substrate surface from the target. The typical growth time for TiO_2 nanowire was 90 min. During depositions, a substrate was heated up to 850 °C by resistive Si heater. After nanowire growth, the substrate temperature was cooled down to room temperature within 30 min. For comparisons, we have fabricated SnO_2 nanowires on Al_2O_3 (110) single crystal substrate and MgO nanowires on MgO (100) single crystal substrate.

Characterization Methods. The surface morphology of fabricated TiO_2 nanowire was evaluated by a field-emission scanning electron microscopy (JEOL, JSM-7001F) at the acceleration voltage of 30 kV. All images were undertaken from a 60° tilted angle if no specific notification was mentioned. The crystalline structure and composition of TiO_2 nanowire were analyzed by a transmission electron microscopy (JEOL, JEM-ARM200F) with integrated energy dispersive spectroscopy (EDS) at the acceleration voltage of 200 kV. Cu mesh covered with a carbon film was utilized to support nanowire samples for TEM measurements. Selected area electron diffraction (SAED) is performed to analyze the crystal structure. To examine quantitatively the material flux of metal species, film depositions at room temperature were carried out at various laser ablation conditions in an Ar atmosphere. This is because in the low-temperature conditions the re-evaporation events at the substrate surface are negligible. After measuring the thickness of obtained thin film by a surface profiler (Alpha-Step IQ), the material flux of Ti was then estimated by using the density of metal element.

RESULTS AND DISCUSSION

Figure 1 shows the typical microscopy images and structural data of successfully fabricated TiO_2 nanowires on a sapphire (110) substrate. The fabrication conditions are the oxygen partial pressure of 10^{-2} Pa and the laser energy of 50 mJ. TEM, SAED, and EDS measurements reveal that the fabricated TiO_2 nanowire is a single crystalline nanostructure with the presence of Au catalyst at the tip, highlighting the occurrence of VLS growth for the present TiO_2 nanowires. SEM image shows the preferential growth of nanowires along 2-fold symmetric orientation. The cross angle between the nanowire growth direction and a sapphire (110) surface was found to be around 57°. This angle almost corresponds to an angle between ⟨001⟩ direction and {101} facets—57.2° in rutile TiO_2. This trend can be interpreted in terms of the small lattice mismatch (0.55%) between rutile TiO_2 (101) and sapphire (110), as illustrated in Figure 2. This result implies the ⟨001⟩ oriented growth direction of obtained TiO_2 nanowires. The ⟨001⟩ growth direction of nanowires can be directly confirmed by analyzing HRTEM image and SAED data, as shown in Figure 1c. The averaged lattice space in HRTEM image along the growth direction is 0.29 nm, which is almost consistent with the *d*-value (0.296 nm) of rutile TiO_2 (001) plane. In addition, the ⟨001⟩ oriented growth of our TiO_2 nanowires is further validated by performing an epitaxial growth of TiO_2 nanowires on a TiO_2 single crystal substrate, as shown in Figure 3. In the case of TiO_2 (001) substrate (Figure 3a), all TiO_2 nanowires were grown only along the perpendicular direction to the

dx.doi.org/10.1021/jp308945b | J. Phys. Chem. C 2012, 116, 24367−24372

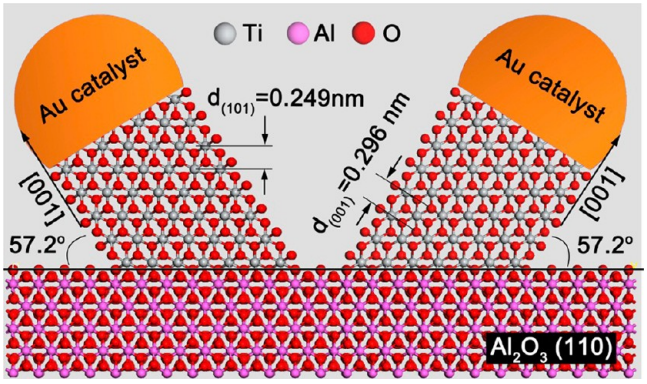

Figure 2. Schematic illustration of the orientation relationship of epitaxial grown TiO_2 nanowires on sapphire (110) substrate. Nanowires grow along rutile ⟨001⟩ direction with an epitaxial plane of (101) with (110) of Al_2O_3 substrate, which exhibits the 2-fold symmetry of nanowire growth.

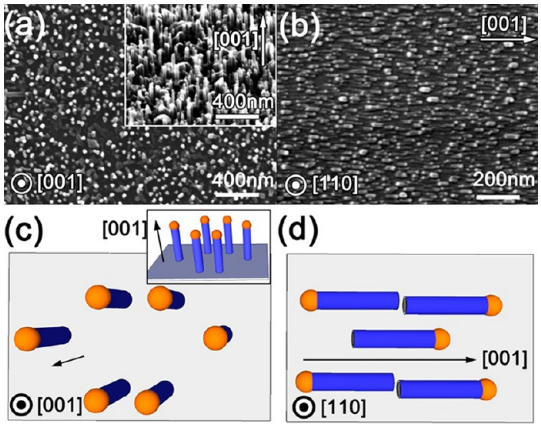

Figure 3. (a) Top view of TiO_2 nanowires grown on rutile TiO_2 (001) substrate. The inset shows the nanowire structure from a 60° tilted observation. (b) Top view of TiO_2 nanowires grown on rutile TiO_2 (110) substrate. (c) Schematic illustration of growth directions of TiO_2 nanowires grown on rutile TiO_2 (001). (d) Schematic illustration of growth directions of TiO_2 nanowires grown on (110) substrates.

substrate surface. On the other hand, in the case of TiO_2 (110) substrate (Figure 3b), nanowires grew along the direction parallel to the substrate surface. Thus, all these experimental results consistently demonstrate that the present TiO_2 nanowires grow along ⟨001⟩ direction with mainly the {110} facets of nanowire surface. Interestingly, this ⟨001⟩ oriented growth direction of TiO_2 nanowires differs from a typical ⟨110⟩ oriented growth direction of TiO_2 nanowires formed by the vapor-phase method.[13,15,16]

Since a surface energy of {110} plane is the lowest in TiO_2 crystal planes, e.g., {110} (0.47 J/m^2) < {100} (0.60 J/m^2) < {101} (0.95 J/m^2) < {001} (1.21 J/m^2),[26−29] the previously reported ⟨110⟩ growth direction seems to be consistent with a scenario based on a minimum free energy at the growth interface (i.e., liquid−solid (LS) interface for VLS growth). Clearly, this existing scenario is not applicable to our ⟨001⟩ oriented TiO_2 nanowires. Since the side wall planes of our TiO_2 nanowires are mainly {110}, as shown in TEM, SAED, and epitaxial data, a scenario based on a minimum free energy at the side wall surface of nanowires (i.e., vapor−solid (VS) interface) seems to be able to explain our present results with {110} surfaces. This ⟨001⟩ oriented growth direction of TiO_2 nanowires has been mainly observed for hydrothermal synthesis,[10−12] where the side wall of nanowires is obviously surrounded by liquid. One possible scenario, to explain the discrepancy between our ⟨001⟩ growth direction and commonly observed ⟨110⟩ growth direction of TiO_2 nanowires formed by the vapor-phase method, is the nanowire diameter dependence of a minimum free energy of growth system because our TiO_2 nanowires show relatively small diameters less than 10 nm, which are smaller than previously reported size ranges—typically above 50−100 nm. The diameter dependence on growth orientation has been experimentally and theoretically investigated in Si nanowire growth.[30,31] In VLS grown Si nanowires, ⟨111⟩ orientation is the most observable growth direction; however, as the nanowire diameter decreases, ⟨112⟩ and ⟨110⟩ oriented growth direction emerge especially below 20 nm diameter.[30] This trend of altering the growth direction has been interpreted in terms of a minimum free energy in all interfaces, including LS interface, VS interface at the side wall, and LV interface of the metal catalyst.[23] If the similar effect exists even for a VLS growth of TiO_2 nanowire, the growth direction might be altered from LS interface dominated ⟨110⟩ growth direction to VS interface dominated ⟨001⟩ growth direction. To validate this scenario, we have examined the metal catalyst diameter dependence on the growth direction of TiO_2 nanowires, as shown in Figure 4. We have varied the thickness

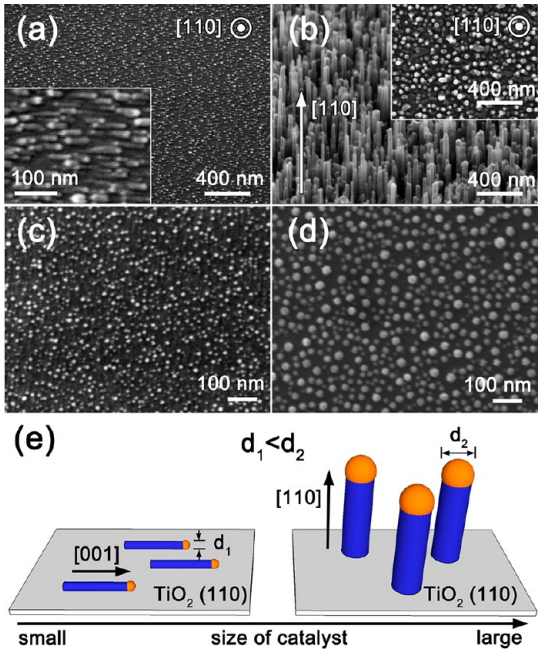

Figure 4. (a, b) Effect of catalyst diameter size on the growth direction. SEM images of TiO_2 nanowires grown on rutile TiO_2 (110) substrate. The data of Au deposition time 3 and 7 s are shown for the comparison. Insets show the magnified top views. (c, d) SEM images of Au catalysts on TiO_2 (110) substrate when varying Au catalyst sizes. (e) Schematic illustration of the catalyst diameter dependence on the growth direction of VLS grown TiO_2 nanowire.

of Au catalysts to change the catalyst diameter, as shown in Figure 4c,d. In Figure 4b, when increasing the diameter of Au catalysts, the TiO_2 nanowires grown in TiO_2 (110) substrate were grown along the direction perpendicular to the substrate surface, which clearly differs from the results for smaller sized Au catalysts in Figure 4a. This result demonstrates that increasing the catalyst diameter alters the growth direction of

dx.doi.org/10.1021/jp308945b | J. Phys. Chem. C 2012, 116, 24367−24372

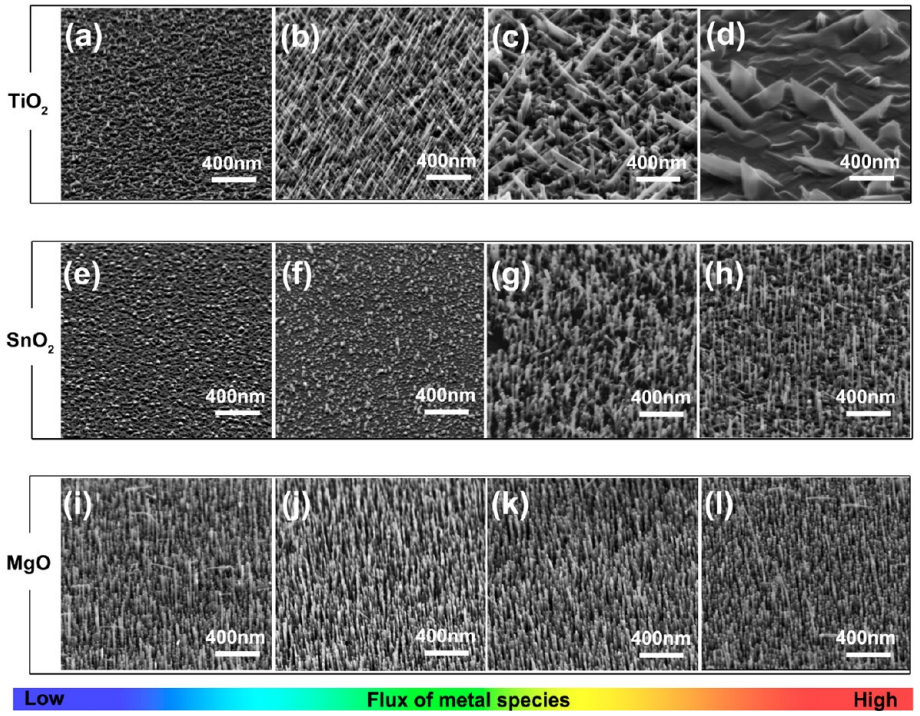

Figure 5. (a–d) SEM images of TiO_2 nanowire grown under various laser energies of (a) 40, (b) 50, (c) 60, and (d) 70 mJ, with a fixed oxygen partial pressure of 1×10^{-2} Pa. (e–h) SEM images of SnO_2 nanowire grown under the laser energies of (e) 40, (f) 50, (g) 60 and (h) 70 mJ, with a fixed oxygen partial pressure of 1×10^{-1} Pa. (i–l) SEM images of MgO nanowire grown under the laser energies of (i) 40, (j) 50, (k) 60, and (l) 70 mJ, with a fixed oxygen partial pressure of 1×10^{-2} Pa.

TiO_2 nanowires from ⟨001⟩ to ⟨110⟩ direction. As illustrated in Figure 4e, for relatively small diameter sizes of catalysts, having {110} VS interface with {001} LS interface (i.e., growth direction for VLS growth) is the most preferred to minimize a total free energy, whereas for larger size ranges ⟨110⟩ growth direction can most efficiently minimize a total free energy due to large LS interface areas. Thus, our present results as to ⟨001⟩ growth direction can be interpreted in terms of a growth mode dominated by a minimum free energy at a nanowire surface.

Next we show that above successful VLS growths of TiO_2 nanowires require a precise control of material flux compared with conventional VLS oxides. The term "VLS oxides" is defined as oxide materials whose nanowires are easily grown by VLS mechanism. Figure 5a–d shows the effect of metal species flux (by varying the laser energy) on the morphology variation of TiO_2 nanostructures deposited onto a sapphire (110) substrate. The fabrication temperature is 850 °C, and the oxygen partial pressure is 10^{-2} Pa. For comparison, results of SnO_2 nanowires on Al_2O_3 (110) substrate under 10^{-1} Pa of oxygen partial pressure and MgO nanowires grown on a MgO (001) substrate under 10^{-2} Pa of oxygen partial pressure are also shown in Figure 5e–h and Figure 5i–l, respectively. TiO_2 nanostructures exhibit a nanowire-like morphology above the laser energy of 50 mJ (Ti flux around $5.0 \times 10^{16}/cm^2$ s) and the oxygen partial pressure of 10^{-2} Pa. The occurrence of VLS growth was already discussed in Figure 1b as a TEM image with the presence of catalyst at the tip. Below the oxygen partial pressure of 10^{-2} Pa, only film-like morphology emerged and any nanowires were not observable. The diameter of nanowires tends to be larger as increasing the material flux of Ti, as can be seen in Figure 5c,d. The nanowire morphology tends to be a cone shape from pillar shape. This tapering is mainly caused by the occurrence of vapor–solid (VS) growth,[32−37] which is detrimental for a VLS growth. In contrast to these TiO_2 nanostructures, MgO nanostructures showed only the nanowire morphology for all material flux conditions employed. The growth window of SnO_2 nanowires is wider than that of TiO_2 nanowires but narrower than that of MgO nanowires. Thus, a VLS grown TiO_2 nanowire can only emerge within a quite narrow range of material flux compared with conventional VLS oxide–SnO_2 and MgO nanowires. To specify more quantitatively such narrow window of material flux for VLS grown TiO_2 nanowires, Figure 6 shows the nanowire density mapping when varying Ti flux and oxygen partial pressure. The mapping data clearly demonstrate the narrow window for a VLS growth of TiO_2 nanowires, and therefore the precise material flux control has been required.

Here we question what essentially determines the narrow window of material flux for a VLS growth of TiO_2 nanowires and also why there is a huge difference among TiO_2, SnO_2, and MgO on the material flux dependence of VLS growth. Within the framework of VLS principles, an occurrence of condensation at a vapor–solid interface (i.e., VS growth) is highly detrimental to promote only a VLS growth.[38] This is because an occurrence of VS growth prevents an area selective crystal growth underneath catalysts. Our previous theoretical study for VLS has identified that a material flux plays a major role on emerging only VLS growth mode rather than VS growth due to a difference between a LS interface and a VS interface on a critical nucleation size.[38] Therefore, we investigate a VS growth rate by measuring a film thickness in the absence of catalysts to extract the nature of VLS grown TiO_2 nanowires. Figure 7a,b shows measured VS growth rates when varying a material flux including a Ti flux and an oxygen partial pressure. In addition, a comparison between TiO_2 and MgO is also shown to manifest the material dependence.

dx.doi.org/10.1021/jp308945b | J. Phys. Chem. C 2012, 116, 24367–24372

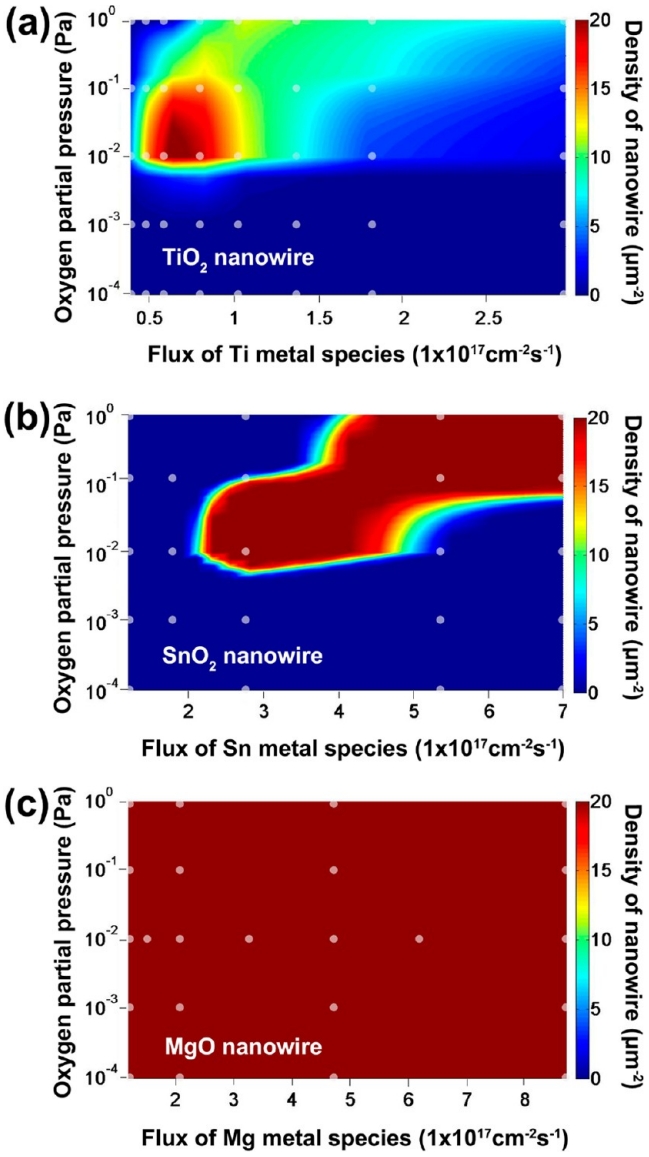

Figure 6. Nanowire density mapping data of (a) TiO_2, (b) SnO_2, and (c) MgO nanowires when varying the supply of metal species and oxygen partial pressure. The gray points indicates the conditions which we performed experiments. The comparison clearly highlights that a VLS growth of TiO_2 nanowires requires a much narrow range of material flux compared with typical VLS oxide—SnO_2 and MgO.

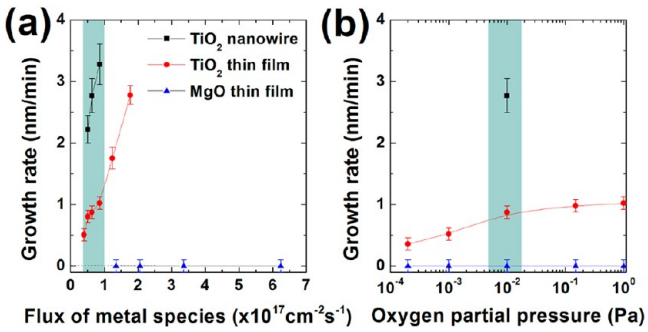

Figure 7. (a) Comparison between TiO_2 and MgO on the film growth rate (VS growth rate) when varying a flux of metal species at constant temperature of 850 °C and constant oxygen pressure of 10^{-2} Pa. The VLS growth rate of TiO_2 nanowires is also shown. (b) Comparison between TiO_2 and MgO on the film growth rate (VS growth rate) when varying an oxygen partial pressure at constant temperature of 850 °C and constant metal flux of $(1.8–2.1) \times 10^{17}$ cm^{-2} s^{-1}. In both (a) and (b), the gray area corresponds to the optimal nanowire growth window, where the TiO_2 nanowire density is over 15 nanowires/μm^2. On the contrary, MgO nanowires are formable all over the experimental conditions.

The clearest feature in Figure 7 is the absence of a VS growth in MgO for all experimental conditions whereas a VS growth of TiO_2 clearly exists. In other words, a condensation of MgO at VS interface can be avoidable, while suppressing condensation for TiO_2 at VS interface seems to be rather difficult within current experimental ranges. This remarkable discrepancy is due to a large difference between Ti and Mg on their equilibrium vapor pressures. For example, for current experimental conditions, 850 °C, a equilibrium vapor pressure of Ti is 3.1×10^{-10} Pa, which is much lower than the equilibrium vapor pressure of Mg, 9.4×10^{3} Pa. In fact, the absence of condensation process at the VS interface for Mg source allows us to fabricate VLS grown MgO nanowires for relatively wide range of material flux in terms of the VLS principle.[38] This must be also same for other conventional VLS oxides including ZnO, SnO_2, and In_2O_3 because the equilibrium vapor pressures of their metal elements are also relatively high. On the other hand, the occurrence of VS growth for TiO_2 system strongly limits a window of material flux for VLS growth. This is because increasing a material flux promotes a VS growth due to an enhanced supersaturation at a VS interface, which results in suppressing a VLS growth via preventing a material collection into catalysts. In an ideal VLS growth, since a VS growth is negligible, increasing a material flux can only contribute a supersaturation at a LS interface, allowing an area selective crystal growth underneath catalysts. On the other hand, in the coexistence of VS and VLS growths, optimizing strictly a window of material flux is essential to realize a VLS growth rate higher than a VS growth rate. Thus, controlling a material flux is intrinsically required to realize a VLS growth of TiO_2 system in the presence of VS growth.

These comparisons between TiO_2 system and conventional VLS oxides highlight that the presence of VS growth in TiO_2 system due to the intrinsic low equilibrium vapor pressure of Ti can reasonably explain why there is a narrow window of material flux for a VLS growth of TiO_2 nanowires. These implications also propose that increasing an operation temperature might be a promising way to suppress a VS growth of TiO_2 and enhance a VLS growth. Another possibility might be the use of metal—organic source with a higher equilibrium vapor pressure for Ti supply. Thus, our results present a strategy based on the fundamental principles rather than a rule of thumb to design and control a VLS growth of single crystalline TiO_2 nanowires.

CONCLUSIONS

We have demonstrated a critical role of material flux on a TiO_2 single crystalline nanowire by the VLS mechanism. We show that a VLS growth of TiO_2 nanowires can emerge only within a quite narrow range of material flux, which is a sharp contrast to typical VLS oxides including MgO, SnO_2, In_2O_3, and ZnO, where their available material flux ranges are much wider. We reveal that a condensation of Ti atoms at a vapor—solid interface, which is detrimental for VLS, is essential to explain a narrow window of material flux for TiO_2 nanowires. In addition, we found that our rutile-TiO_2 nanowires preferentially

dx.doi.org/10.1021/jp308945b | J. Phys. Chem. C 2012, 116, 24367–24372

grow along ⟨001⟩ direction, which interestingly differs from a typical ⟨110⟩ oriented growth in previous reports. The ⟨001⟩ growth direction can be interpreted in terms of a growth mode dominated by a minimum free energy at a nanowire surface when a TiO_2 nanowire diameter is small.

AUTHOR INFORMATION

Corresponding Author

*E-mail: yanagi32@sanken.osaka-u.ac.jp (T.Y.); kawai@sanken.osaka-u.ac.jp (T.K.).

Notes

The authors declare no competing financial interest.

ACKNOWLEDGMENTS

This study was in part supported by a Grant-in-Aid for Scientific Research on Innovative Areas [20111004] from the Ministry of Education, Culture Sports, Science and Technology (MEXT) of Japan. A part of this work was supported by "Low-Carbon Research Network (Handai satellite)" of Ministry of Education, Culture, Sports, Science and Technology (MEXT), Japan. F.Z., B.X., G.M., and Y.H. were supported by NEXT. T.K. and S.R. were supported by the FIRST program.

REFERENCES

(1) Asahi, R.; Morikawa, T.; Ohwaki, T.; Aoki, K.; Taga, Y. *Science* **2001**, *293*, 269−271.
(2) Kawai, T.; Sakata, T. *Nature* **1979**, *282*, 283−284.
(3) Oregan, B.; Gratzel, M. *Nature* **1991**, *353*, 737−740.
(4) Kuwauchi, Y.; Yoshida, H.; Akita, T.; Haruta, M.; Takeda, S. *Angew. Chem., Int. Ed.* **2012**, *51*, 7729−7733.
(5) Diebold, U. *Surf. Sci. Rep.* **2003**, *48*, 53−229.
(6) Cass, M. J.; Walker, A. B.; Martinez, D.; Peter, L. M. *J. Phys. Chem. B* **2005**, *109*, 5100−5107.
(7) Shankar, K.; Basham, J. I.; Allam, N. K.; Varghese, O. K.; Mor, G. K.; Feng, X. J.; Paulose, M.; Seabold, J. A.; Choi, K. S.; Grimes, C. A. *J. Phys. Chem. C* **2009**, *113*, 6327−6359.
(8) Lei, Y.; Zhang, L. D.; Meng, G. W.; Li, G. H.; Zhang, X. Y.; Liang, C. H.; Chen, W.; Wang, S. X. *Appl. Phys. Lett.* **2001**, *78*, 1125−1127.
(9) Peng, X. S.; Chen, A. C. *Adv. Funct. Mater.* **2006**, *16*, 1355−1362.
(10) Wang, H. E.; Chen, Z. H.; Leung, Y. H.; Luan, C. Y.; Liu, C. P.; Tang, Y. B.; Yan, C.; Zhang, W. J.; Zapien, J. A.; Bello, I.; Lee, S. T. *Appl. Phys. Lett.* **2010**, *96*, 263104.
(11) Liu, B.; Aydil, E. S. *J. Am. Chem. Soc.* **2009**, *131*, 3985−3990.
(12) Feng, X. J.; Shankar, K.; Varghese, O. K.; Paulose, M.; Latempa, T. J.; Grimes, C. A. *Nano Lett.* **2008**, *8*, 3781−3786.
(13) Kim, M. H.; Baik, J. M.; Zhang, J. P.; Larson, C.; Li, Y. L.; Stucky, G. D.; Moskovits, M.; Wodtke, A. M. *J. Phys. Chem. C* **2010**, *114*, 10697−106702.
(14) Richter, C.; Schmuttenmaer, C. A. *Nat. Nanotechnol.* **2010**, *5*, 769−772.
(15) Wu, J. M.; Shih, H. C.; Wu, W. T. *Nanotechnology* **2006**, *17*, 105−109.
(16) Lee, J. C.; Park, K. S.; Kim, T. G.; Choi, H. J.; Sung, Y. M. *Nanotechnology* **2006**, *17*, 4317−4321.
(17) Nagashima, K.; Yanagida, T.; Tanaka, H.; Kawai, T. *J. Appl. Phys.* **2007**, *101*, 124304.
(18) Nagashima, K.; Yanagida, T.; Tanaka, H.; Seki, S.; Saeki, A.; Tagawa, S.; Kawai, T. *J. Am. Chem. Soc.* **2008**, *130*, 5378−5382.
(19) Marcu, A.; Yanagida, T.; Nagashima, K.; Oka, K.; Tanaka, H.; Kawai, T. *Appl. Phys. Lett.* **2008**, *92*, 173119.
(20) Oka, K.; Yanagida, T.; Nagashima, K.; Tanaka, H.; Kawai, T. *J. Am. Chem. Soc.* **2009**, *131*, 3434−3435.
(21) Klamchuen, A.; Yanagida, T.; Nagashima, K.; Seki, S.; Oka, K.; Taniguchi, M.; Kawai, T. *Appl. Phys. Lett.* **2009**, *95*, 053105.
(22) Oka, K.; Yanagida, T.; Nagashima, K.; Tanaka, H.; Seki, S.; Honsho, Y.; Ishimaru, M.; Hirata, A.; Kawai, T. *Appl. Phys. Lett.* **2009**, *95*, 133110.
(23) Nagashima, K.; Yanagida, T.; Oka, K.; Taniguchi, M.; Kawai, T.; Kim, J. S.; Park, B. H. *Nano Lett.* **2010**, *10*, 1359−1363.
(24) Oka, K.; Yanagida, T.; Nagashima, K.; Kawai, T.; Kim, J. S.; Park, B. H. *J. Am. Chem. Soc.* **2010**, *132*, 6634−6635.
(25) Nagashima, K.; Yanagida, T.; Oka, K.; Kanai, M.; Klamchuen, A.; Kim, J. S.; Park, B. H.; Kawai, T. *Nano Lett.* **2011**, *11*, 2114−2118.
(26) Tafen, D.; Lewis, J. P. *Phys. Rev. B* **2009**, *80*, 014104.
(27) Barnard, A. S.; Zapol, P.; Curtiss, L. A. *J. Chem. Theory Comput.* **2005**, *1*, 107−116.
(28) Evarestov, R. A.; Migas, D. B.; Zhukovskii, Y. F. *J. Phys. Chem. C* **2012**, *116*, 13395−13402.
(29) Migas, D. B.; Shaposhnikov, V. L.; Borisenko, V. E.; D'Avitaya, F. A. *J. Phys. Chem. C* **2010**, *114*, 21013−21019.
(30) Schmidt, V.; Senz, S.; Gosele, U. *Nano Lett.* **2005**, *5*, 931−935.
(31) Wang, C. X.; Hirano, M.; Hosono, H. *Nano Lett.* **2006**, *6*, 1552−1555.
(32) Nagashima, K.; Yanagida, T.; Tanaka, H.; Kawai, T. *Appl. Phys. Lett.* **2007**, *90*, 233103.
(33) Yanagida, T.; Nagashima, K.; Tanaka, H.; Kawai, T. *Appl. Phys. Lett.* **2007**, *91*, 061502.
(34) Nagashima, K.; Yanagida, T.; Oka, K.; Tanaka, H.; Kawai, T. *Appl. Phys. Lett.* **2008**, *93*, 153103.
(35) Yanagida, T.; Marcu, A.; Matsui, H.; Nagashima, K.; Oka, K.; Yokota, K.; Taniguchi, M.; Kawai, T. *J. Phys. Chem. C* **2008**, *112*, 18923−18926.
(36) Suzuki, M.; Hidaka, Y.; Yanagida, T.; Kanai, M.; Kawai, T.; Kai, S. *Phys. Rev. E* **2010**, *82*, 011605.
(37) Klamchuen, A.; Yanagida, T.; Kanai, M.; Nagashima, K.; Oka, K.; Kawai, T.; Suzuki, M.; Hidaka, Y.; Kai, S. *Appl. Phys. Lett.* **2010**, *97*, 073114.
(38) Suzuki, M.; Hidaka, Y.; Yanagida, T.; Klamchuen, A.; Kanai, M.; Kawai, T.; Kai, S. *Phys. Rev. E* **2011**, *83*, 061606.